THE JOURNAL OF BIOLOGICAL CHEMISTRY
Vol. 278, No. 26, Issue of June 27, pp. 23868–23873, 2003

Printed in U.S.A.

The 1.5-Å Structure of *Chryseobacterium meningosepticum* Zinc β-Lactamase in Complex with the Inhibitor, D-Captopril*

Received for publication, January 31, 2003, and in revised form, April 4, 2003
Published, JBC Papers in Press, April 8, 2003, DOI 10.1074/jbc.M301062200

Isabel García-Sáez‡, Julie Hopkins‡, Cyril Papamicael§, Nicola Franceschini¶, Gianfranco Amicosante¶, Gian Maria Rossolini‖, Moreno Galleni, Jean-Marie Frère**, and Otto Dideberg‡ ‡‡**

*From the ‡Laboratoire de Cristallographie Macromoléculaire, Institut de Biologie Structurale Jean-Pierre Ebel (CNRS-Commissariat à l'Energie Atomique (Saclay, France)), 41, rue Jules Horowitz, F-38027 Grenoble Cedex 1, France, §Oxford Center for Molecular Sciences, England, South Parks Rd., GB-OXFORD, OX1 3QY, United Kingdom, ¶Dipartimento di Scienze e Tecnologie Biomediche, Università di L'Aquila, I-67100 L'Aquila, Italy, ‖Dipartimento di Biologia Moleculare, Sezione di Microbiologia, Università di Siena, I-53100 Siena, Italy, and **Laboratoire d'Enzymologie, Centre d'Ingénierie des Protéines, Institut de Chimie, Université de Liège, Sart Tilman, B-4000 Liège, Belgium*

The crystal structure of the class-B β-lactamase, BlaB, from the pathogenic bacterium, *Chryseobacterium meningosepticum*, in complex with the inhibitor, D-captopril, has been solved at 1.5-Å resolution. The enzyme has the typical αβ/βα metallo-β-lactamase fold and the characteristic two metal binding sites of members of the subclass B1, in which two Zn^{2+} ions were identified. D-Captopril, a diastereoisomer of the commercial drug, captopril, acts as an inhibitor by displacing the catalytic hydroxyl ion required for antibiotic hydrolysis and intercalating its sulfhydryl group between the two Zn^{2+} ions. Interestingly, D-captopril is located on one side of the active site cleft. The x-ray structure of the complex of the closely related enzyme, IMP-1, with a mercaptocarboxylate inhibitor, which also contains a sulfhydryl group bound to the two Zn^{2+} ions, shows the ligand to be located on the opposite side of the active site cleft. A molecule generated by fusion of these two inhibitors would cover the entire cleft, suggesting an interesting approach to the design of highly specific inhibitors.

Antibiotic resistance of pathogenic bacteria is a major clinical concern because it has increased significantly during recent years, rendering antimicrobial therapy progressively less effective. One mechanism by which bacteria can escape the action of antibiotics is the production of metallo-β-lactamases (MBLs)[1] or class B β-lactamases (1). These enzymes were initially described as a curiosity in innocuous strains of *Bacillus cereus* (2) but were subsequently identified in several pathogenic species responsible for human infections in which the enzymes are either encoded by resident chromosomal genes or by horizontally acquired genes carried on mobile genetic elements (3–7). Class B β-lactamases have a broad spectrum of substrates, including penicillin, cephalosporin, and carbapenem, some of which are not substrates for active site serine β-lactamases (3, 4). At present no inhibitors of these enzymes are used clinically, making them a potential source of antibiotic resistance.

The MBL family has been divided into three different subclasses, B1, B2, and B3, on the basis of sequence similarities (8). MBLs have two metal binding sites (the His site, or first site, and the Cys site, or second site), which bind Zn^{2+} ions required for enzyme activity. In general, both the mono-Zn^{2+} (Zn^{2+} in the His site) and di-Zn^{2+} forms are active but have different kinetic properties (9, 10); the exception is CphA from *Aeromonas hydrophilia,* which is inhibited by the presence of the second zinc ion (11). In the mono-Zn^{2+} enzyme, a water-mediated mechanism for the hydrolysis of the antibiotic β-lactam ring has been suggested in which a water molecule is activated by the presence of the Zn^{2+} ion in the His site, then carries out nucleophilic attack against the carbonyl carbon of the β-lactam. Residues Asp-120 and Cys-221 from the second site would help keep the active water molecule in position. Asp-120 would also act as a general base, transferring the proton from the water molecule to the nitrogen atom of the β-lactam ring, causing bond cleavage and opening of the ring, leading to inactivation of the antibiotic (12, 13). In the bi-Zn^{2+} enzyme, a hydroxide ion is positioned close to the two Zn^{2+} ions. The second Zn^{2+} would also help to anchor Asp-120 (14) and would orient the β-lactam ring by binding to the β-lactam nitrogen of the antibiotic (15). Although both the mono- and di-Zn^{2+} forms exist, it has been hypothesized that only the mono-Zn^{2+} form is present under normal physiological conditions (16).

Because of the great interest in MBL inhibition, several classes of inhibitors have been described (17, 18); these include phenazines (19), ketone derivatives of L- and D-alanine and trifluoromethyl alcohol (20), thioesters (21, 22), biphenyl tetrazoles (23, 24), amino acid-derived hydroxamates (25), thiols (26–30), and tricyclic natural products (31). However, despite many of these having good inhibitory properties, only a few thiols have a broad spectrum of inhibition for MBLs. In this context, the analysis of the three-dimensional structures of MBLs in complex with potential inhibitors becomes a powerful tool for rational drug design. At present, the structures of *Bacteroides fragilis* CcrA complexed with Mes, biphenyl

* This work was supported by European Union Human and Mobility Grant HPRN-CT-2002-00264 and Belgian Government Grant PAI P5/33. The costs of publication of this article were defrayed in part by the payment of page charges. This article must therefore be hereby marked "*advertisement*" in accordance with 18 U.S.C. Section 1734 solely to indicate this fact.

The atomic coordinates and structure factors (code 1m2x) have been deposited in the Protein Data Bank, Research Collaboratory for Structural Bioinformatics, Rutgers University, New Brunswick, NJ (http://www.rcsb.org/).

‡‡ To whom correspondence should be addressed. Tel.: 33-4-38-78-56-09; Fax: 33-4-38-78-54-94; E-mail: otto@ibs.fr.

[1] The abbreviations used are: MBL, metallo-β-lactamase; Mes, 4-morpholineethanesulfonic acid.

tetrazole, or a tricyclic natural product (32) and of (23, 31) *Pseudomonas aeruginosa* IMP-1 complexed with mercaptocarboxylate (30) or with succinic acid derivatives (33) have been reported.

BlaB is a chromosome-encoded MBL produced by *Chryseobacterium meningosepticum*. It is a member of subclass B1 has a broad substrate profile (34–36) and is produced constitutively (37). *C. meningosepticum* is an ubiquitous Gram-negative rod bacterium of clinical relevance because it can cause neonatal meningitis, adult septicemia, and nosocomial infections and is resistant to most β-lactams, including carbapenems (38, 39).

D-Captopril (1-(D-3-mercapto-2-methylpropionyl)-D-proline) is a diastereoisomer of the commercial drug captopril (1-(D-3-mercapto-2-methylpropionyl)-L-proline), used clinically to control high blood pressure. It acts as an angiotensin-converting enzyme inhibitor and increases plasma level of the vasodilator, bradykinin (40). D-Captopril, which was synthesized to test its inhibitory effect on MBLs, is a good competitive inhibitor of BlaB (K_i = 70–100 μM) at neutral pH.[2] In this work, we describe the first high resolution (1.5 Å) three-dimensional structure of BlaB complexed with D-captopril.

EXPERIMENTAL PROCEDURES

Synthesis of D-Captopril—D-Captopril was synthesized from commercially available compounds, starting with D-proline (41, 42). The final hydrolysis reaction was carried out using 1 N NaOH under an argon atmosphere.

Expression, Purification, and Crystallization of the D-Captopril Complex—The overexpression, purification, and characterization of the protein have been described (34). For crystallization, the hanging drop method was used. Crystals were obtained by mixing 2 μl of protein (5 mg/ml in 10 mM sodium cacodylate, 100 μM zinc acetate, 100 μM dithiothreitol, pH 6.5) and 1 μl of the reservoir solution (28% polyethylene glycol 4000, 0.2 M sodium acetate, and 0.1 M Tris-HCl, pH 8.4) at 8 °C; crystals appeared after approximately 3 weeks. A crystal was soaked for ~5 weeks in previously equilibrated drops of the reservoir solution containing 2 mM D-captopril, then the crystal was flash-cooled in liquid nitrogen using precipitant containing 15% glycerol as cryoprotectant and stored in liquid nitrogen for subsequent data collection at a synchrotron source.

Data Collection and Processing—Diffraction data sets were collected at the ID14–4 beamline of the European Synchrotron Radiation Facility in Grenoble, France. A data set of 360 frames at λ = 0.9792 Å was collected at 1.5-Å resolution with 0.5° oscillation steps. Data integration performed using DENZO/SCALEPACK (43) gave an initial ambiguity in the space group determination, since according to the automated indexing procedure, the crystal could be cubic or trigonal, with similar distortion indexes. The data were re-indexed using DENZO/SCALEPACK and scaled using SCALA (44), trying different space groups to solve this ambiguity. After this stage, the crystal was considered to be cubic I23 or $I2_13$, with $a = b = c$ = 112.85 Å, $\alpha = \beta = \gamma = 90°$, R_{sym} = 0.117 (1 molecule/asymmetric unit), or trigonal R3, with $a = b$ = 159.69 Å, c = 97.82 Å, $\alpha = \beta = 90°$, $\gamma = 120°$, R_{sym} = 0.119 (3 or 4 molecules/asymmetric unit) (Table I).

Structural Determination and Refinement—The structure of the MBL, BcII, from *B. cereus* at 1.8-Å resolution (45) with no ions or water molecules was used as a model for molecular replacement using the program AMoRe (46). Because the x-ray data could be indexed in three space groups ($I2_13$, I23, and R3), various tests were performed. In brief, data indexed in R3 were used successfully in AMoRe with a BcII model performing a four molecule/asymmetric unit search (c-factor = 36.3%, R-factor = 48.0%). With these solutions and using a noncrystallographic symmetry-averaging map calculated using the CNS program (47), a partial model of BlaB was built using TURBO (48). A full model of BlaB at 1.5 Å was made using ARP/WARP (49). From the initial ($2F_o - F_c$) and ($F_o - F_c$) maps, the inhibitor, D-captopril, was localized close to the Zn^{2+} ions in the active site. Further cycles of energy minimization, B-factor refinement, and water picking were performed using CNS programs (47). Models for D-captopril were not included until their conformations were well defined by the unbiased $|F_o - F_c|$, ϕ_{calc} electron density maps. D-Captopril molecules in each of the four monomers were modeled. The model was refined without any non-crystallographic-symmetry restrains, yielding $R_{working}$ = 18.95% and R_{free} = 20.76%.

TABLE I
X-ray data collection and structure refinement of BlaB

Data collection from the synchrotron source European Synchrotron Radiation Facility, Grenoble, France beam-line 1D14–4.

Data collection statistics	
Unit cell parameters	$a = b$ = 159.7 Å, c = 97.8 Å $\alpha = \beta = 90°$, $\gamma = 120°$
Space group	R3
Molecules/asymmetric unit	4
Max. resolution (Å)	1.5
No. of unique reflections	138,708
Overall completeness (%)	90
Last shell completeness (%)[a]	90
Multiplicity	2.6
R_{sym}[b]	0.12 (0.18)[a]
Refinement statistics	
No. of reflections[c]	133860
No. of atoms (non H)	8047
$R_{working}$[d] (%)	18.9
R_{free}[e] (%)	20.8
Root mean square deviation from ideal	
Bonds (Å)	0.005
Angles (°)	1.26
Average B factor (Å^2)	
Protein	15.0
D-Captopril	15.6
Ramachandran plot (%)	
Most favored	89.3
Allowed	9.2
Generously allowed	0.5
Disallowed	1.0

[a] Last resolution shell 1.58–1.50 Å.
[b] $R_{sym} = \Sigma|I_j^- \langle 1\rangle|/\Sigma \langle I\rangle$, where I_j is the intensity for reflection j, and $\langle I\rangle$ is the mean intensity.
[c] no σ cutoff.
[d] $R_{working} = \Sigma \; ||F_o| - |F_c||/\Sigma|F_o|$, calculated with the working set.
[e] R_{free} was calculated similarly using 10% of the data excluded from the calculation for $R_{working}$.

RESULTS

The BlaB monomer shares a structural feature with other members of the MBL family, an αβ/βα fold, in which a compact core of two β-sheets is surrounded by α-helices (Fig. 1). The crystal, which shows a cubic pseudo-symmetry, belongs to the space group R3 and has four monomers per asymmetric unit (A, B, C, and D).

The four monomers are practically identical, with a few local differences due to slightly different environments or to effects of crystal packing (*e.g.* monomers A, B, and D are missing the last four C-terminal residues, whereas monomer C is missing the last six). The root mean square deviation between the conserved Cα atoms of the four molecules is about 0.1 Å. The active site of BlaB shares a feature with other subclass B1 structures, namely that two Zn^{2+} ions (Zn1 and Zn2) occupy the two metal binding sites, the His site (His-116, His-118, His-196) and the Cys site (Asp-120, Cys-221, His-263) (Fig. 2, *a* and *c*). A clear electron density corresponding to a molecule of D-captopril was found close to the active site. The inhibitor intercalates its sulfhydryl group between the two Zn^{2+} ions (distance S-Zn1, 2.32 Å; S-Zn2, 2.30 Å in monomer A) (Fig. 2). The sulfur atom is also close to the NE2 of His-196 (3.34 Å) (Table II). The inhibitor is located in the positively charged groove leading to the active site (Fig. 3*a*) and is present in the four molecules/asymmetric unit with full occupancy.

Other interactions enhance the binding of the inhibitor molecule. The carboxylic group of D-captopril is stabilized by hydrogen bonds between its O_2 and the NZ of Lys-167 and two water molecules; the other carboxylic oxygen, O3, is bound to the amide main chain of Asp-119. The O1 carbonyl oxygen of

[2] H. W. Adolph, personal communication.

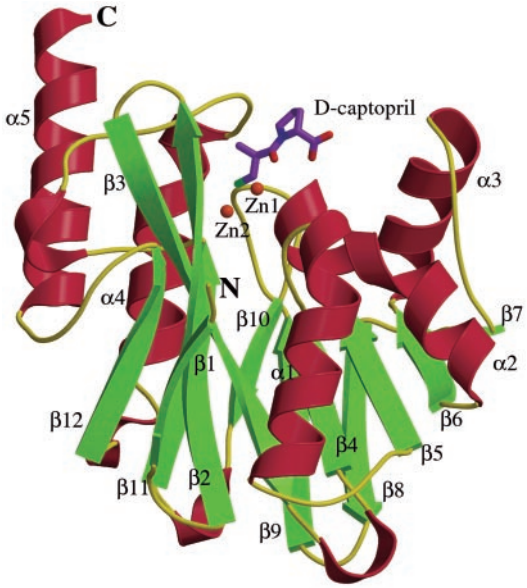

FIG. 1. **Structure of BlaB in complex with D-captopril.** Three-dimensional structure of BlaB from *C. meningosepticum* in complex with D-captopril. α-Helices, β-Strands, and loops are shown in *red*, *green*, and *yellow*, respectively. Zn^{2+} ions are represented as *dark orange* spheres. The N and C termini are labeled. The figure was produced using MOLSCRIPT (53).

the inhibitor also makes a hydrogen bond with another water molecule (Fig. 2*b*). In addition, the inhibitor is stabilized by several hydrophobic contacts between its carbons and His-118, Asp-120, and Tyr-233 (Fig. 2*b* and Table II).

DISCUSSION

Structural Comparisons—The sequence of BlaB shows 25-35% identity with those of other subclass B1 β-lactamases. The secondary structure topology of the four available x-ray structures (BcII, CcrA, BlaB, and IMP-1) is very similar, the only difference being that the first short β-strand seen in BcII and CcrA is absent in BlaB and IMP-1. Pairwise superposition of the C_α atoms of BlaB and BcII (1BMC), Ccra (1ZNB), or IMP-1 (1JJE) gives a root mean difference density of 1.5, 1.4, and 1.9 Å, respectively.

In subclass B1, there is a loop between β2 and β3 (residues 61–65), which is disordered in the structure of native BcII (12). However, in the presence of an inhibitor, the loop is stabilized (30), transforming the active site groove into a tunnel-shaped cavity. In the BlaB structure, the loop is also well defined, probably due to the presence of D-captopril in the active site (Fig. 2*c*). Interestingly, D-captopril has no direct interaction with any residues in the loop (Fig. 2, *b* and *c*; Table II). The flexibility in the loop may help to accommodate the inhibitor, which itself may help to stabilize the loop. This stabilization takes place indirectly by Trp-87, which makes a double hydrogen bond between its NE1 and the OD1 of Asp-119 and the water molecule that hydrogen bonds to the O1 carbonyl oxygen of D-captopril (Table II). Trp-87 also makes hydrophobic contacts with the active site residue, His-263. All these interactions determine the position of Trp-87, which establishes hydrophobic interactions between its ring and two residues, Phe-61 and Asn-59. The loop is strongly stabilized by hydrogen bonds between the carbonyl oxygens and the amide nitrogens of the backbone of this region (amino acids 57–69). In the apical part of the loop facing the solvent, a water molecule forms a bridge between the ND2 of Asn-62 and the carbonyl oxygen of Phe-61, which also makes a hydrogen bond with the amide backbone of Thr-64. In addition, the amide backbone of Phe-61

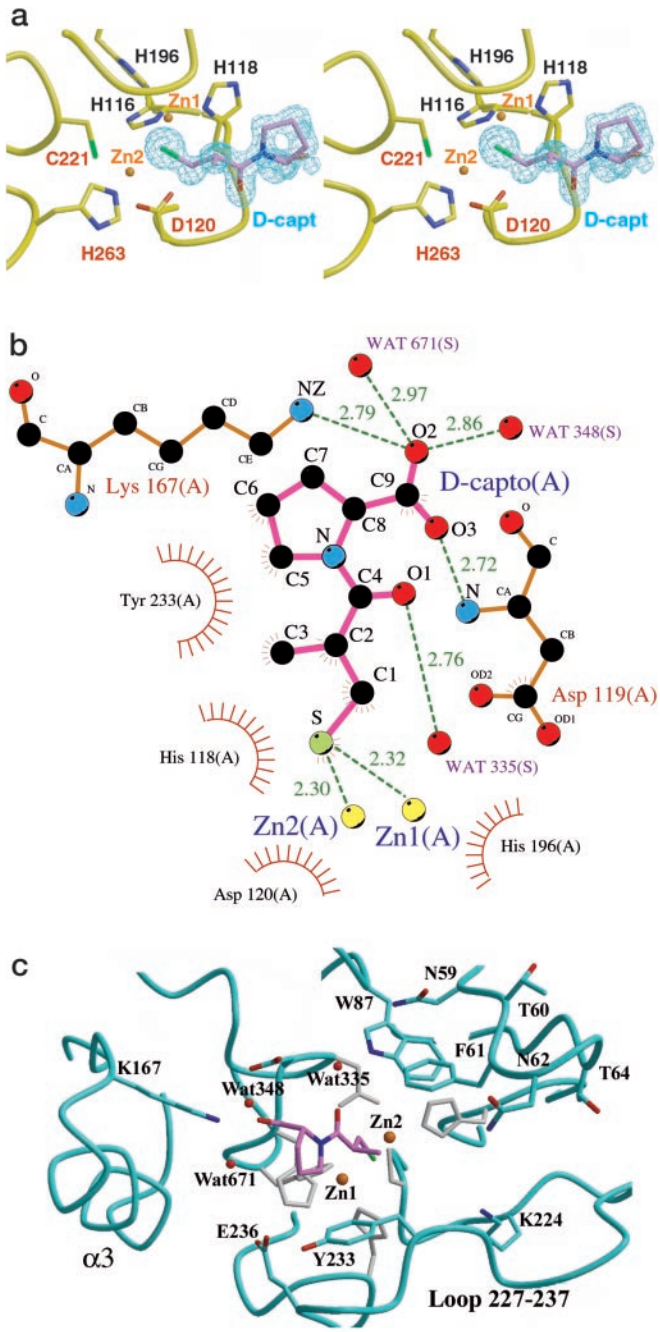

FIG. 2. **Coordination of D-captopril by BlaB.** *a*, stereoview of the active site of BlaB in complex with D-captopril. The calculated $F_o - F_c$ map at 1.5 σ shows the presence of the inhibitor. The inhibitor atoms were not included in the phase calculation. The residues labeled in *black* belong to the His site, and those in *red* belong to the Cys site. Zinc ions are represented as *brown spheres*. The figure was produced using BOBSCRIPT (54). *b*, protein-ligand interactions between BlaB and D-captopril depicted in monomer A using LIGPLOT (55). In the *schematic* drawing, strong interactions are shown as *dashed green lines*. Ligand and protein hydrophobic contacts are represented as *curved red combs*. *c*, active site cleft of BlaB. Zinc ions and water molecules are represented in *brown* and *red spheres*, respectively. D-Captopril is displayed in *sticks* (carbon, nitrogen, and sulfur atoms colored in *violet*, *blue*, and *green*, respectively). Amino acid residues cited in the text under "Structural Comparisons" are labeled, and Zn^{2+} ligands are colored in *gray*.

makes hydrogen bonds with the carbonyl oxygen of the main chain of Thr-64. A second water molecule makes hydrogen bonds with this bridging water molecule and the hydroxyl group of Tyr-67. In BlaB, the loop appears to be closer to the

TABLE II
Interactions between BlaB and D*-captopril (≤3.5 Å)*
Parentheses represent the water molecule numbering in the structure.

D-Captopril	Monomer	A	B	C	D
O_2	CG D119	3.50	3.49	3.49	3.39
	OD1 D119	3.45	3.31	3.39	3.29
	OD2 D119	3.31	3.46	3.35	3.29
	NZ K167	2.79	2.86	2.78	2.85
	Water	(348) 2.86	(606) 2.88	(590) 2.91	(502) 2.93
	Water	(671) 2.97	(698) 2.96		
C9	CG D119	3.44	3.46	3.46	3.45
	OD1 D119		3.39	3.46	3.47
	NZ K167			3.49	
O_3	CA H118	3.10	3.13	3.10	3.08
	CB H118	3.19	3.23	3.20	3.15
	C H118	3.40	3.40	3.41	3.39
	N D119	2.72	2.71	2.74	2.73
	CG D119	3.42	3.42	3.47	3.49
	OD2 D119	3.43			
	NZ K167			3.49	
C5	CD2 Y233	3.44	3.47	3.48	3.46
	CE2 Y233	3.31	3.33	3.33	3.34
O1	Water	(335) 2.76	(450) 2.78	(468) 2.77	(285) 2.74
C1	CB H118		3.50	3.49	3.49
	OD1 D120	3.28	3.24	3.25	3.21
	Zn1	3.24	3.19	3.25	3.22
	Zn2	3.37	3.41	3.42	3.35
S	NE2 H196	3.34	3.37	3.33	3.35
	Zn1	2.32	2.33	2.34	2.36
	Zn2	2.30	2.31	2.34	2.27

rest of the protein than in the other three structures, with the hydrophobic residues, Phe-61, Tyr-67, and Trp-87, pointing toward the inside of the protein and creating a hydrophobic environment even though the loop does not interact directly with the inhibitor. In addition, the loops in BlaB and BcII are in different positions, *e.g.* the distance between equivalent residues in BlaB and BcII is 5.44 Å for Phe-61 and 5.77 Å for Asn-62. Interestingly, in subclass B1 MBLs, bulky hydrophobic residues are often found at positions 61, 67, and 87. In all MBL structures, the Asp or Asn residue at residue 84 has an φ angle outside the allowed range ($\varphi \sim 60 \pm 1°$) and plays an important structural role, contributing to the architecture of the active site. Of the residues that are highly conserved and/or potentially involved in substrate binding in subclass B1 β-lactamases, three positions are particularly interesting in the BlaB structure, 224, 233, and 236 (Fig. 2*c*).

Lys-224 is very well defined in the electron density map (NZ, B factor of 13.5 $Å^2$). The NZ makes three hydrogen bonds with the carbonyl oxygen of the preceding amino acid (Ile-223) and two water molecules. Lys-224 is assumed to interact with the carboxyl group of the β-lactam antibiotic (30). However, Lys-224 is not found in subclass B3 MBLs, and no equivalent residue is observed in a similar spatial position in the L1 (15) or FEZ-1 structures (50).

Based on x-ray crystallographic structures, Asn-233 and Zn1 were thought to form an oxyanion hole to polarize the carbonyl group of the β-lactam antibiotic (50, 51). In BlaB, Asn-233 is replaced by Tyr, and the hydroxyl of the tyrosine is 7.88 Å away from Zn1 (Fig. 2*c*). Interestingly, Glu-236, which is an aspartic acid residue in the BcII, CcrA, and IMP-1 enzymes, makes three hydrogen-bonds with OH Tyr-233, NEZ His-118 (a zinc ligand), and a water molecule, whereas Asp-236 in the other three x-ray structures only hydrogen-bonds to NEZ His-118 and a water molecule. Consequently, no oxyanion hole is observed in the present structure. However, the observed position of Tyr-233 could be the result of complex formation, since C_3, C_5, and C_6 of D-captopril make hydrophobic contacts with the tyrosine side chain. Nevertheless, rotation around χ_1 is sterically forbidden, and only a large conformational change of the 227–237 loop (Fig. 2*c*) upon substrate binding could bring OH Tyr-233 or other side chain residues into positions where they could form part of the oxyanion hole.

Binding of the Inhibitor—The main interaction between BlaB and D-captopril occurs through intercalation of the sulfur atom of the inhibitor between the two Zn^{2+} ions, leading to the removal of the activated water (OH^- group) (Fig. 2, *a* and *b*; Table II). A similar situation has been seen in the three-dimensional structure of IMP-1 in complex with a mercaptocarboxylate inhibitor (2-mercaptomethyl-4-phenyl-butyrylimino)-(5-tetrazol-1-ylmethyl-thiophen-2-yl)-acetic acid) (30).

Structural superposition of the structures of the two protein-inhibitor complexes shows that the inhibitors intercalate their sulfur groups almost identically between the two Zn^{2+} ions of the active site. A striking observation is that, although they are located in different parts of the active site, together the two inhibitors cover the entire active site cavity (Fig. 3*a*). The fusion of these two inhibitor molecules could be a good starting point for generating a new family of more effective inhibitors (Fig. 3*b*). Based on the structural superposition using this new molecule, many interactions would be retained, including those between the S atom and the two Zn^{2+} ions, the carboxylate groups and the main-chain amide nitrogens (N119 and N233), the carboxylate groups and the NZ of two lysines (Lys-167 and Lys-224), and many hydrophobic contacts.

In the crystal structure of IMP-1 complexed with a succinic acid derivative (33), one oxygen of the carboxylic group of the inhibitor is located between the two Zn^{2+} ions, displacing the hydroxyl. Curiously, in the three-dimensional structure of the subclass B3 MBL FEZ-1 complexed with D-captopril (50), the inhibitor is not located in the active site, because a sulfate ion from the crystallization solution intercalates one of its oxygen atoms between the two Zn^{2+} ions. In the complex of *B. fragilis* CcrA with a biphenyl tetrazole (23), the tetrazole ring of the inhibitor acts as an extra ligand for the second Zn^{2+}, changing its coordination and provoking a distortion of the active site and the removal of the water molecules from the active site.

Taking together our results and all currently known three-dimensional structures of MBLs complexed with inhibitors (23, 30, 32, 33), we can conclude that there is a high variability in

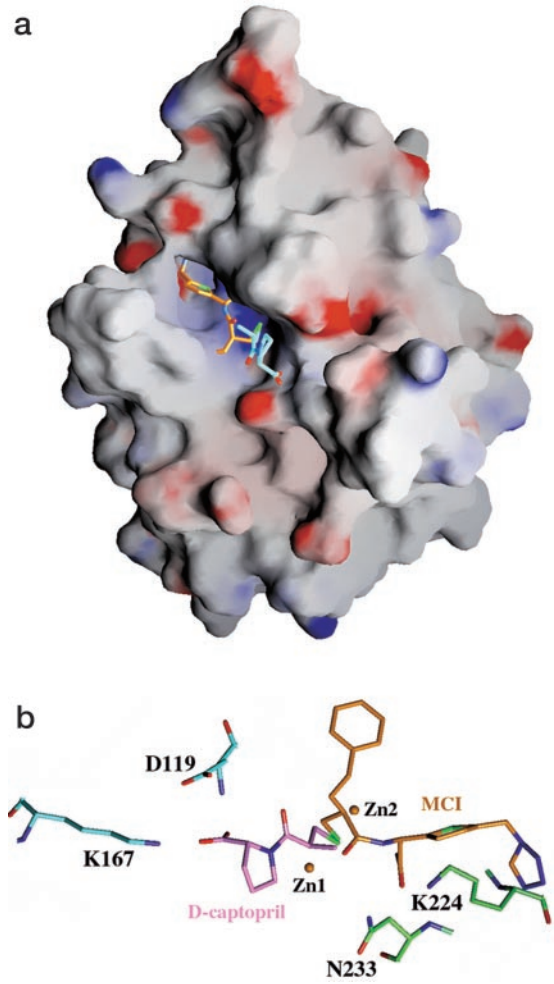

FIG. 3. **Two inhibitors in the active site cleft.** *a*, GRASP representation (52) of BlaB complexed with both D-captopril (carbons colored in *sky blue*) and the mercaptocarboxylate inhibitor (carbons colored in *orange*) from the IMP-1 complex (30) after structural superposition of the BlaB and IMP-1 structures. Both molecules intercalate their sulfur atoms between the two zinc atoms of the active site but are localized in different areas of the active site cavity. *b*, close-up view of the two inhibitors showing strong interactions between the two inhibitors and BlaB.

the modes of binding of the inhibitors depending on the β-lactamase sequence and the size and chemical properties of the inhibitor. However, one feature is constant, which is the intercalation of a charged group between the Zn^{2+} ions and the removal of the bridging hydroxide directly involved in water-mediated hydrolysis of the substrate. Moreover, the new BlaB structure presented here highlights the structural diversity in the MBL family. The evolution of broad substrate profile enzymes, such as BlaB, poses a serious threat to antibacterial therapy, and a detailed analysis of inhibitor-enzyme complexes is vital for the design of new inhibitors.

Acknowledgment—We thank Dr. E. Gordon for help with the beamline ID-14-4 at the European Synchrotron Radiation Facility, Grenoble, France.

REFERENCES

1. Ambler, R. P., Daniel, M., Fleming, J., Hermoso, J. M., Pang, C., and Waley, S. G. (1985) *FEBS Lett.* **189,** 207–211
2. Kubawara, S., and Abraham, E. P. (1967) *Biochem. J.* **103,** 27–30
3. Rasmussen, B. A., and Bush, K. (1997) *Antimicrob. Agents Chemother.* **41,** 223–232
4. Bush, K. (1998) *Clin. Infect. Dis.* **27,** Suppl. 1, 48–53
5. Senda, K., Arakawa, Y., Ichiyama, S., Nakashima, K., Ito, H., Ohsuka, S., Shimokata, K., Kato, N., and Ohta, M. (1996) *J. Clin. Microbiol.* **34,** 2909–2913
6. Laraki, N., Galleni, M., Thamm, I., Riccio, M. L., Amicosante, G., Frère, J.-M., and Rossolini, G. M. (1999) *Antimicrob. Agents Chemother.* **43,** 890–901
7. Lauretti, L., Riccio, M. L., Mazzariol, A., Cornaglia, G., Amicosante, G., Fontana, R., and Rossolini, G. M. (1999) *Antimicrob. Agents Chemother.* **43,** 1584–1590
8. Galleni, M., Lamotte-Brasseur, J., Rossolini, G. M., Spencer, J., Dideberg, O., and Frère, J.-M. (2001) *Antimicrob. Agents Chemother.* **45,** 660–663
9. Paul-Soto, R., Hernandez-Valladares, M., Galleni, M., Bauer, R., Zeppezauer, M., Frère, J.-M., and Adolph, H. W. (1998) *FEBS Lett.* **438,** 137–140
10. Paul-Soto, R., Bauer, R., Frère, J.-M., Galleni, M., Meyer-Klaucke, W., Nolting, H., Rossolini, G. M., de Seny, D., Hernandez-Valladares, M., Zeppezauer, M., and Adolph, H. W. (1999) *J. Biol. Chem.* **274,** 13242–13249
11. Hernandez-Valladares, M., Felici, A., Weber, G., Adolph, H. W., Zeppezauer, M., Rossolini, G. M., Amicosante, G., Frère, J.-M., and Galleni, M. (1997) *Biochemistry* **36,** 11534–11541
12. Carfi, A., Parès, S., Duée, E., Galleni, M., Duez, C., Frère, J.-M., and Dideberg, O. (1995) *EMBO J.* **14,** 4914–4921
13. Diaz, N., Suarez, D., and Merz, K. M. J. (2001) *J. Am. Chem. Soc.* **123,** 9867–9879
14. Rasia, R. M., and Vila, A. J. (2002) *Biochemistry* **41,** 1853–1860
15. Ullah, J. H., Walsh, T. R., Taylor, I. A., Emery, D. C., Verma, C. S., Gamblin, S. J., and Spencer, J. (1998) *J. Mol. Biol.* **284,** 125–136
16. Wommer, S., Rival, S., Heinz, U., Galleni, M., Frère, J.-M., Franceschini, N., Amicosante, G., Rasmussen, B., Bauer, R., and Adolph, H. W. (2002) *J. Biol. Chem.* **277,** 24142–24147
17. Di Modugno, E., and Felici, A. (1999) *Curr. Opin. Anti-Infective Investig. Drugs* **1,** 26–39
18. Payne, D. J., Du, W., and Bateson, J. H. (2000) *Expert Opin. Investig. Drugs* **9,** 247–261
19. Gilpin, M. L., Fulston, M., Payne, D., Cramp, R., and Hood, I. (1995) *J. Antibiot.* (*Tokyo*) **48,** 1081–1085
20. Walter, M. W., Felici, A., Galleni, M., Soto, R. P., Adlington, R. M., Baldwin, J. E., Frère, J.-M., Gololobov, M., and Schofield, C. J. (1996) *Bioorg. Med. Chem. Lett.* **6,** 2455–2458
21. Payne, D. J., Bateson, J. H., Gasson, B. C., Khushi, T., Proctor, D., Pearson, S. C., and Reid, R. (1997) *FEMS Microbiol. Lett.* **157,** 171–175
22. Greenlee, M. L., Laub, J. B., Balkovec, J. M., Hammond, M. L., Hammond, G. G., Pompliano, D. L., and Epstein-Toney, J. H. (1999) *Bioorg. Med. Chem. Lett.* **9,** 2549–2554
23. Toney, J. H., Fitzgerald, P. M., Grover-Sharma, N., Olson, S. H., May, W. J., Sundelof, J. G., Vanderwall, D. E., Cleary, K. A., Grant, S. K., Wu, J. K., Kozarich, J. W., Pompliano, D. L., and Hammond, G. G. (1998) *Chem. Biol.* (*Lond.*) **5,** 185–196
24. Toney, J. H., Cleary, K. A., Hammond, G. G., Yuan, X., May, W. J., Hutchins, S. M., Ashton, W. T., and Vanderwall, D. E. (1999) *Bioorg. Med. Chem. Lett.* **9,** 2741–2746
25. Walter, M. W., Valladares, M. H., Adlington, R. M., Amicosante, G. M., Baldwin, J. E., Frère, J.-M., Galleni, M., and Rossolini, G. M. (1999) *Bioorg. Chem.* **27,** 35–40
26. Goto, M., Takahashi, T., Yamashita, F., Koreeda, A., Mori, H., Ohta, M., and Arakawa, Y. (1997) *Biol. Pharm. Bull* **20,** 1136–1140
27. Page, M. I., and Laws, A. P. (1998) *J. Chem. Soc. Chem. Commun.* **10,** 1609–1618
28. Scrofani, S. D., Chung, J., Huntley, J. J., Benkovic, S. J., Wright, P. E., and Dyson, H. J. (1999) *Biochemistry* **38,** 14507–14514
29. Yang, K. W., and Crowder, M. W. (1999) *Arch. Biochem. Biophys.* **368,** 1–6
30. Concha, N. O., Janson, C. A., Rowling, P., Pearson, S., Cheever, C. A., Clarke, B. P., Lewis, C., Galleni, M., Frère, J.-M., Payne, D. J., Bateson, J. H., and Abdel-Meguid, S. S. (2000) *Biochemistry* **39,** 4288–4298
31. Payne, D. J., Hueso-Rodriguez, J. A., Boyd, H., Concha, N. O., Janson, C. A., Gilpin, M., Bateson, J. H., Cheever, C., Niconovich, N. L., Pearson, S., Rittenhouse, S., Tew, D., Diez, E., Perez, P., De La Fuente, J., Rees, M., and Rivera-Sagredo, A. (2002) *Antimicrob. Agents Chemother.* **46,** 1880–1886
32. Fitzgerald, P. M. D., Wu, J. K., and Toney, J. H. (1998) *Biochemistry* **37,** 6791–6800
33. Toney, J. H., Hammond, G. G., Fitzgerald, P. M., Sharma, N., Balkovec, J. M., Rouen, G. P., Olson, S. H., Hammond, M. L., Greenlee, M. L., and Gao, Y. D. (2001) *J. Biol. Chem.* **276,** 31913–31918
34. Rossolini, G. M., Franceschini, N., Riccio, M. L., Mercuri, P. S., Perilli, M., Galleni, M., Frère, J.-M., and Amicosante, G. (1998) *Biochem. J.* **332,** 145–152
35. Bellais, S., Poirel, L., Leotard, S., Naas, T., and Nordmann, P. (2000) *Antimicrob. Agents Chemother.* **44,** 3028–3034
36. Woodford, N., Palepou, M. F., Babini, G. S., Holmes, B., and Livermore, D. M. (2000) *Antimicrob. Agents Chemother.* **44,** 1448–1452
37. Bloch, K. C., Nadarajah, R., and Jacobs, R. (1997) *Medicine* (*Baltimore*) **76,** 30–41
38. von Graevenitz, A. (1995) *Manual of Clinical Microbiology* (Murray, P. R., Baron, E. J., Pfaller, M. A., Tenover, F. C., and Yolken, R. H., eds) 6th Ed, pp. 520–532, American Society for Microbiology, Washington, D. C.
39. Fraser, S. L., and Jorgensen, J. H. (1997) *Antimicrob. Agents Chemother.* **41,** 2738–2741
40. Smith, W. H., and Ball, S. G. (2000) *Basic Res. Cardiol.* **95,** Suppl. 1, 8–14
41. Suh, J. T., Skiles, J. W., Williams, B. E., Youssefyeh, R. D., Jones, H., Loev, B., Neiss, E. S., Scwab, A., Mann, W. S., Khandwala, A., Wolf, P. S., and Weinryb, I. (1985) *J. Med. Chem.* **28,** 57–66
42. Skiles, J. W., Suh, J. T., Williams, B. E., Menard, P. R., Barton, J. N., Loev, B., Jones, H., Neiss, E. S., Schwab, A., Mann, W. S., Khandwala, A., Wolf, P. S., and Weinryb, I. (1986) *J. Med. Chem.* **29,** 784–796
43. Otwinowski, Z., and Minor, W. (1997) *Methods Enzymol.* **276,** 307–326
44. CCP4 (1994) *Acta Crystallogr. Sect. D* **50,** 760–763
45. Carfi, A., Duée, E., Galleni, M., Frère, J.-M., and Dideberg, O. (1998) *Acta Crystallogr. Sect. D* **54,** 313–323
46. Navaza, J. (1994) *Acta Crystallogr. Sect. A* **50,** 157–163

47. Brünger, A. T., Adams, P. D., Clore, G. M., DeLano, W. L., Gros, P., Grosse-Kunstleve, R. W., Jiang, J. S., Kuszewski, J., Nilges, M., Pannu, N. S., Read, R. J., Rice, L. M., Simonson, T., and Warren, G. L. (1998) *Acta Crystallogr. Sect. D* **54,** 905–921
48. Roussel, A., and Cambillau, C. (1991) *Silicon Graphics Geometry Partners Directory 88*, Mountain View, CA
49. Perrakis, A., Sixma, T. K., Wilson, K. S., and Lamzin, V. S. (1997) *Acta Crystallogr. Sect. D* **53,** 448–455
50. Garcia-Sáez, I., Mercuri, P. S., Papamicael, C., Kahn, R., Frère, J.-M., Galleni, M., Rossolini, G. M., and Dideberg, O. (2003) *J. Mol. Biol.* **325,** 651–660
51. Concha, N. O., Rasmussen, B. A., Bush, K., and Herzberg, O. (1996) *Structure (Lond.)* **4,** 823–836
52. Nicholls A. (1992) *GRASP: Graphical Representation and Analysis of Surface Properties*, Columbia University, New York
53. Kraulis, P. J. (1991) *J. Appl. Crystallogr.* **24,** 946–950
54. Esnouf, R. M. (1999) *Acta Crystallogr. Sect. D* **55,** 938–940
55. Wallace, A. C., Laskowski, R. A., and Thornton, J. M. (1995) *Protein Eng.* **8,** 127–134

Protein Structure and Folding:

The 1.5-Å Structure of *Chryseobacterium meningosepticum* Zinc β-Lactamase in Complex with the Inhibitor, D-Captopril

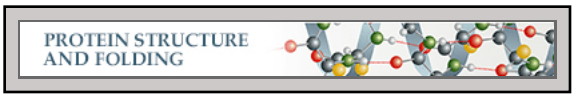

Isabel García-Sáez, Julie Hopkins, Cyril Papamicael, Nicola Franceschini, Gianfranco Amicosante, Gian Maria Rossolini, Moreno Galleni, Jean-Marie Frère and Otto Dideberg

J. Biol. Chem. 2003, 278:23868-23873.
doi: 10.1074/jbc.M301062200 originally published online April 8, 2003
